12

MULTICHANNEL AND MULTICARRIER SYSTEMS

In some applications, it is desirable to transmit the same information-bearing signal over several channels. This mode of transmission is used primarily in situations where there is a high probability that one or more of the channels will be unreliable from time to time. For example, radio channels such as ionospheric scatter and tropospheric scatter suffer from signal fading due to multipath, which renders the channels unreliable for short periods of time. As another example, multichannel signaling is sometimes employed in military communication systems as a means of overcoming the effects of jamming of the transmitted signal. By transmitting the same information over multiple channels, we are providing signal diversity, which the receiver can exploit to recover the information.

Another form of multichannel communications is multiple carrier transmission, where the frequency band of the channel is subdivided into a number of subchannels and information is transmitted on each of the subchannels. A rationale for subdividing the frequency band of a channel into a number of narrowband channels is given below.

In this chapter, we consider both multichannel signal transmission and multicarrier transmission. We begin with a treatment of multichannel transmission.

12-1 MULTICHANNEL DIGITAL COMMUNICATION IN AWGN CHANNELS

In this section, we confine our attention to multichannel signaling over fixed channels that differ only in attenuation and phase shift. The specific model for

the multichannel digital signaling system may be described as follows. The signal waveforms, in general are expressed as

$$s_m^{(n)}(t) = \text{Re}\,[s_{lm}^{(n)}(t)e^{j2\pi f_n t}], \quad 0 \le t \le T$$
$$n = 1, 2, \ldots, L, \quad m = 1, 2, \ldots, M \quad (12\text{-}1\text{-}1)$$

where L is the number of channels and M is the number of waveforms. The waveforms are assumed to have equal energy and to be equally probable a priori. The waveforms $\{s_m^{(n)}(t)\}$ transmitted over the L channels are scaled by the factors $\{\alpha_n\}$, phase-shifted by $\{\phi_n\}$, and corrupted by additive noise. The equivalent lowpass signals received from the L channels may be expressed as

$$r_l^{(n)}(t) = \alpha_n e^{j\phi_n} s_{lm}^{(n)}(t) + z_n(t), \quad 0 \le t \le T$$
$$n = 1, 2, \ldots, L, \quad m = 1, 2, \ldots, M \quad (12\text{-}1\text{-}2)$$

where $\{s_{lm}^{(n)}(t)\}$ are the equivalent lowpass transmitted waveforms and $\{z_n(t)\}$ represent the additive noise processes on the L channels. We assume that $\{z_n(t)\}$ are mutually statistically independent and identically distributed gaussian noise random processes.

We consider two types of processing at the receiver, namely, coherent detection and noncoherent detection. The receiver for coherent detection estimates the channel parameters $\{\alpha_n\}$ and $\{\phi_n\}$ and uses the estimates in computing the decision variables. Suppose we define $g_n = \alpha_n e^{-j\phi_n}$ and let $\hat{g}_n$ be the estimate of g_n. The multichannel receiver correlates each of the L received signals with a replica of the corresponding transmitted signals, multiplies each of the correlator outputs by the corresponding estimates $\{\hat{g}_n^*\}$, and sums the resulting signals. Thus, the decision variables for coherent detection are the correlation metrics

$$CM_m = \sum_{n=1}^{L} \text{Re}\left[\hat{g}_n^* \int_0^T r_l^{(n)}(t) s_{lm}^{(n)*}(t)\, dt\right], \quad m = 1, 2, \ldots, M \quad (12\text{-}1\text{-}3)$$

In noncoherent detection, no attempt is made to estimate the channel parameters. The demodulator may base its decision either on the sum of the envelopes (envelope detection) or the sum of the squared envelopes (square-law detection) of the matched filter outputs. In general, the performance obtained with envelope detection differs little from the performance obtained with square-law detection in AWGN. However, square-law detection of multichannel signaling in AWGN channels is considerably easier to analyze than envelope detection. Therefore, we confine our attention to square-law detection of the received signals of the L channels, which produces the decision variables

$$CM_m = \sum_{n=1}^{L} \left| \int_0^T r_l^{(n)}(t) s_{lm}^{(n)*}(t)\, dt \right|^2, \quad m = 1, 2, \ldots, M \quad (12\text{-}1\text{-}4)$$

Let us consider binary signaling first, and assume that $s_{l1}^{(n)}$, $n = 1, 2, \ldots, L$

are the L transmitted waveforms. Then an error is committed if $CM_2 > CM_1$, or, equivalently, if the difference $D = CM_1 - CM_2 < 0$. For noncoherent detection, this difference may be expressed as

$$D = \sum_{n=1}^{L} (|X_n|^2 - |Y_n|^2) \tag{12-1-5}$$

where the variables $\{X_n\}$ and $\{Y_n\}$ are defined as

$$\begin{aligned} X_n &= \int_0^T r_l^{(n)}(t) s_{l1}^{(n)*}(t)\, dt, \qquad n = 1, 2, \ldots, L \\ Y_n &= \int_0^T r_l^{(n)}(t) s_{l2}^{(n)*}(t)\, dt, \qquad n = 1, 2, \ldots, L \end{aligned} \tag{12-1-6}$$

The $\{X_n\}$ are mutually independent and identically distributed gaussian random variables. The same statement applies to the variables $\{Y_n\}$. However, for any n, X_n and Y_n may be correlated. For coherent detection, the difference $D = CM_1 - CM_2$ may be expressed as

$$D = \tfrac{1}{2} \sum_{n=1}^{L} (X_n Y_n^* + X_n^* Y_n) \tag{12-1-7}$$

where, by definition,

$$\begin{aligned} Y_n &= \hat{g}_n, \qquad n = 1, 2, \ldots, L \\ X_n &= \int_0^T r_l^{(n)}(t)[s_{l1}^{(n)*}(t) - s_{l2}^{(n)*}(t)]\, dt \end{aligned} \tag{12-1-8}$$

If the estimates $\{\hat{g}_n\}$ are obtained from observation of the received signal over one or more signaling intervals, as described in Appendix C, their statistical characteristics are described by the gaussian distribution. Then the $\{Y_n\}$ are characterized as mutually independent and identically distributed gaussian random variables. The same statement applies to the variables $\{X_n\}$. As in noncoherent detection, we allow for correlation between X_n and Y_n, but not between X_m and Y_n for $m \neq n$.

12-1-1 Binary Signals

In Appendix B, we derive the probability that the general quadratic form

$$D = \sum_{n=1}^{L} (A|X_n|^2 + B|Y_n|^2 + CX_n Y_n^* + C^* X_n^* Y_n) \tag{12-1-9}$$

in complex-valued gaussian random variables is less than zero. This probability, which is given in (B-21) of Appendix B, is the probability of error for

binary multichannel signaling in AWGN. A number of special cases are of particular importance.

If the binary signals are antipodal and the estimates of $\{g_n\}$ are perfect, as in coherent PSK, the probability of error takes the simple form

$$P_b = Q(\sqrt{2\gamma_b}) \tag{12-1-10}$$

where

$$\begin{aligned}\gamma_b &= \frac{\mathscr{E}}{N_0}\sum_{n=1}^{L}|g_n|^2 \\ &= \frac{\mathscr{E}}{N_0}\sum_{n=1}^{L}\alpha_n^2\end{aligned} \tag{12-1-11}$$

is the SNR per bit. If the channels are all identical, $\alpha_n = \alpha$ for all n and, hence,

$$\gamma_b = \frac{L\mathscr{E}}{N_0}\alpha^2 \tag{12-1-12}$$

We observe that $L\mathscr{E}$ is the total transmitted signal energy for the L signals. The interpretation of this result is that the receiver combines the energy from the L channels in an optimum manner. That is, there is no loss in performance in dividing the total transmitted signal energy among the L channels. The same performance is obtained as in the case in which a single waveform having energy $L\mathscr{E}$ is transmitted on one channel. This behavior holds true only if the estimates $\hat{g}_n = g_n$, for all n. If the estimates are not perfect, a loss in performance occurs, the amount of which depends on the quality of the estimates, as described in Appendix C.

Perfect estimates for $\{g_n\}$ constitute an extreme case. At the other extreme, we have binary DPSK signaling. In DPSK, the estimates $\{\hat{g}_n\}$ are simply the (normalized) signal-plus-noise samples at the outputs of the matched filters in the previous signaling interval. This is the poorest estimate that one might consider using in estimating $\{g_n\}$. For binary DPSK, the probability of error obtained from (B-21) is

$$P_b = \frac{1}{2^{2L-1}}e^{-\gamma_b}\sum_{n=1}^{L-1}c_n\gamma_b^n \tag{12-1-13}$$

where, by definition,

$$c_n = \frac{1}{n!}\sum_{k=0}^{L-1-n}\binom{2L-1}{k} \tag{12-1-14}$$

and γ_b is the SNR per bit defined in (12-1-11) and, for identical channels in (12-1-12). This result can be compared with the single-channel ($L = 1$) error probability. To simplify the comparison, we assume that the L channels have identical attenuation factors. Thus, for the same value of γ_b, the performance of the multichannel system is poorer than that of the single-channel system. That is, splitting the total transmitted energy among L channels results in a loss in performance, the amount of which depends on L.

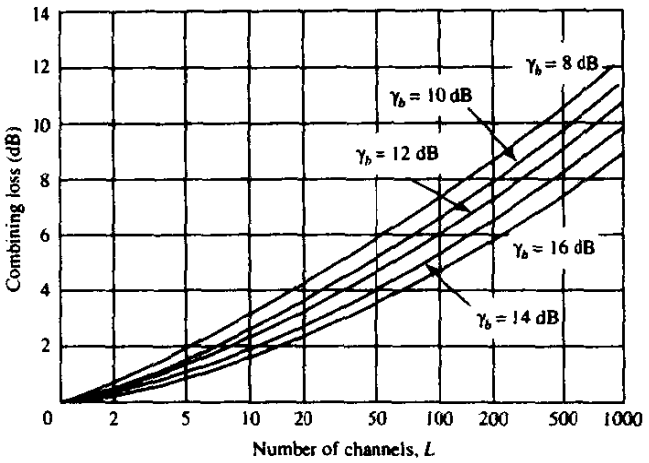

FIGURE 12-1-1 Combining loss in noncoherent detection and combination of binary multichannel signals.

A loss in performance also occurs in square-law detection of orthogonal signals transmitted over L channels. For binary orthogonal signaling, the expression for the probability of error is identical in form to that for binary DPSK given in (12-1-13), except that γ_b is replaced by $\frac{1}{2}\gamma_b$. That is, binary orthogonal signaling with noncoherent detection is 3 dB poorer than binary DPSK. However, the loss in performance due to noncoherent combination of the signals received on the L channels is identical to that for binary DPSK.

Figure 12-1-1 illustrates the loss resulting from noncoherent (square-law) combining of the L signals as a function of L. The probability of error is not shown, but it can be easily obtained from the curve of the expression

$$P_b = \tfrac{1}{2}e^{-\gamma_b} \tag{12-1-15}$$

which is the error probability of binary DPSK shown in Fig. 5-2-12 and then degrading the required SNR per bit, γ_b, by the noncoherent combining loss corresponding to the value of L.

12-1-2 M-ary Orthogonal Signals

Now let us consider M-ary orthogonal signaling with square-law detection and combination of the signals on the L channels. The decision variables are given by (12-1-4). Suppose that the signals $s_1^{(n)}(t)$, $n = 1, 2, \ldots, L$, are transmitted over the L AWGN channels. Then, the decision variables are expressed as

$$\begin{aligned} U_1 &= \sum_{n=1}^{L} |2\mathcal{E}\alpha_n + N_{n1}|^2 \\ U_m &= \sum_{n=1}^{L} |N_{nm}|^2, \qquad m = 2, 3, \ldots, M \end{aligned} \tag{12-1-16}$$

where the $\{N_{nm}\}$ are complex-valued zero-mean gaussian random variables with variance $\sigma^2 = \frac{1}{2}E(|N_{nm}|^2) = 2\mathscr{E}N_0$. Hence U_1 is described statistically as a noncentral chi-square random variable with $2L$ degrees of freedom and noncentrality parameter

$$s^2 = \sum_{n=1}^{L} (2\mathscr{E}\alpha_n)^2 = 4\mathscr{E}^2 \sum_{n=1}^{L} \alpha_n^2 \tag{12-1-17}$$

Using (2-1-118), we obtain the pdf of U_1 as

$$p(u_1) = \frac{1}{4\mathscr{E}N_0}\left(\frac{u_1}{s^2}\right)^{(L-1)/2} \exp\left(-\frac{s^2+u_1}{4\mathscr{E}N_0}\right) I_{L-1}\left(\frac{s\sqrt{u_1}}{2\mathscr{E}N_0}\right), \qquad u_1 \geq 0 \tag{12-1-18}$$

On the other hand, the $\{U_m\}$, $m = 2, 3, \ldots, M$, are statistically independent and identically chi-square-distributed random variables, each having $2L$ degrees of freedom. Using (2-1-110), we obtain the pdf for U_m as

$$p(u_m) = \frac{1}{(4\mathscr{E}N_0)^L(L-1)!} u_m^{L-1} e^{-u_m/4\mathscr{E}N_0}, \qquad u_m \geq 0$$

$$m = 2, 3, \ldots, M \tag{12-1-19}$$

The probability of a symbol error is

$$\begin{aligned} P_M &= 1 - P_c \\ &= 1 - P(U_2 < U_1, U_3 < U_1, \ldots, U_M < U_1) \\ &= 1 - \int_0^\infty [P(U_2 < u_1 \mid U_1 = u_1)]^{M-1} p(u_1)\, du_1 \end{aligned} \tag{12-1-20}$$

But

$$P(U_2 < u_1 \mid U_1 = u_1) = 1 - \exp\left(-\frac{u_1}{4\mathscr{E}N_0}\right) \sum_{k=0}^{L-1} \frac{1}{k!}\left(\frac{u_1}{4\mathscr{E}N_0}\right)^k \tag{12-1-21}$$

Hence,

$$\begin{aligned} P_M &= 1 - \int_0^\infty \left[1 - e^{-u_1/4\mathscr{E}N_0} \sum_{k=0}^{L-1} \frac{1}{k!}\left(\frac{u_1}{4\mathscr{E}N_0}\right)^k\right]^{M-1} p(u_1)\, du_1 \\ &= 1 - \int_0^\infty \left(1 - e^{-v} \sum_{k=0}^{L-1} \frac{v^k}{k!}\right)^{M-1} \left(\frac{v}{\gamma}\right)^{(L-1)/2} e^{-(\gamma+v)} I_{L-1}(2\sqrt{\gamma v})\, dv \end{aligned} \tag{12-1-22}$$

where

$$\gamma = \mathscr{E} \sum_{n=1}^{L} \alpha_n^2 / N_0$$

The integral in (12-1-22) can be evaluated numerically. It is also possible to expand the term $(1-x)^{M-1}$ in (12-1-22) and carry out the integration term by term. This approach yields an expression for P_M in terms of finite sums.

An alternative approach is to use the union bound

$$P_M < (M-1)P_2(L) \tag{12-1-23}$$

where $P_2(L)$ is the probability of error in choosing between U_1 and any one of the $M-1$ decision variables $\{U_m\}$, $m = 2, 3, \ldots, M$. From our previous discussion on the performance of binary orthogonal signaling, we have

$$P_2(L) = \frac{1}{2^{2L-1}} e^{-k\gamma_b/2} \sum_{n=0}^{L-1} c_n (\tfrac{1}{2}k\gamma_b)^n \tag{12-1-24}$$

where c_n is given by (12-1-14). For relatively small values of M, the union bound in (12-1-23) is sufficiently tight for most practical applications.

12-2 MULTICARRIER COMMUNICATIONS

From our treatment of nonideal linear filter channels in Chapters 10 and 11, we have observed that such channels introduce ISI, which degrades performance compared with the ideal channel. The degree of performance degradation depends on the frequency response characteristics. Furthermore, the complexity of the receiver increases as the span of the ISI increases.

Given a particular channel characteristic, the communication system designer must decide how to efficiently utilize the available channel bandwidth in order to transmit the information reliably within the transmitter power constraint and receiver complexity constraints. For a nonideal linear filter channel, one option is to employ a single carrier system in which the information sequence is transmitted serially at some specified rate R symbols/s. In such a channel, the time dispersion is generally much greater than the symbol rate and, hence, ISI results from the nonideal frequency response characteristics of the channel. As we have observed, an equalizer is necessary to compensate for the channel distortion.

An alternative approach to the design of a bandwidth-efficient communication system in the presence of channel distortion is to subdivide the available channel bandwidth into a number of subchannels, such that each subchannel is nearly ideal. To elaborate, suppose that $C(f)$ is the frequency response of a nonideal, band-limited channel with a bandwidth W, and that the power spectral density of the additive gaussian noise is $\Phi_{nn}(f)$. Then, we divide the bandwidth W into $N = W/\Delta f$ subbands of width Δf, where Δf is chosen sufficiently small that $|C(f)|^2/\Phi_{nn}(f)$ is approximately a constant within each subband. Furthermore, we shall select the transmitted signal power to be distributed in frequency as $P(f)$, subject to the constraint that

$$\int_W P(f)\, df \leq P_{\text{av}} \tag{12-2-1}$$

where, P_{av} is the available average power of the transmitter. Let us evaluate the capacity of the nonideal additive gaussian noise channel.

12-2-1 Capacity of a Nonideal Linear Filter Channel

Recall that the capacity of an ideal, band-limited, AWGN channel is

$$C = W \log_2\left(1 + \frac{P_{av}}{WN_0}\right) \tag{12-2-2}$$

where C is the capacity in bits/s, W is the channel bandwidth, and P_{av} is the average transmitted power. In a multicarrier system, with Δf sufficiently small, the subchannel has capacity

$$C_i = \Delta f \log_2\left[1 + \frac{\Delta f P(f_i)\,|C(f)|^2}{\Delta f \Phi_{nn}(f_i)}\right] \tag{12-2-3}$$

Hence, the total capacity of the channel is

$$C = \sum_{i=1}^{N} C_i = \Delta f \sum_{i=1}^{N} \log_2\left[1 + \frac{P(f_i)\,|C(f_i)|^2}{\Phi_{nn}(f_i)}\right] \tag{12-2-4}$$

In the limit as $\Delta f \to 0$, we obtain the capacity of the overall channel in bits/s as

$$C = \int_W \log_2\left[1 + \frac{P(f)\,|C(f)|^2}{\Phi_{nn}(f)}\right] df \tag{12-2-5}$$

Under the constraint on $P(f)$ given by (12-2-1), the choice of $P(f)$ that maximizes C may be determined by maximizing the integral

$$\int_W \left\{\log_2\left[1 + \frac{P(f)\,|C(f)|^2}{\Phi_{nn}(f)}\right] + \lambda P(f)\right\} df \tag{12-2-6}$$

where λ is a Lagrange multiplier, which is chosen to satisfy the constraint. By using the calculus of variations to perform the maximization, we find that the optimum distribution of transmitted signal power is the solution to the equation

$$\frac{1}{|C(f)|^2 P(f) + \Phi_{nn}(f)} + \lambda = 0 \tag{12-2-7}$$

Therefore, $P(f) + \Phi_{nn}(f)/|C(f)|^2$ must be a constant, whose value is adjusted to satisfy the average power constraint in (12-2-1). That is,

$$P(f) = \begin{cases} K - \Phi_{nn}(f)/|C(f)|^2 & (f \in W) \\ 0 & (f \notin W) \end{cases} \tag{12-2-8}$$

This expression for the channel capacity of a nonideal linear filter channel with additive gaussian noise is due to Shannon (1949). The basic interpretation of this result is that the signal power should be high when the channel SNR $|C(f)|^2/\Phi_{nn}(f)$ is high, and low when the channel SNR is low. This result on

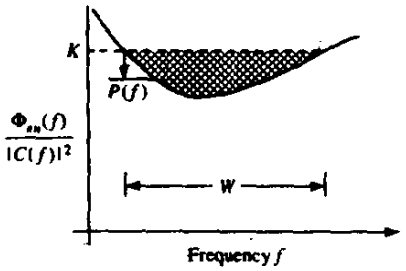

FIGURE 12-2-1 The optimum water-pouring spectrum.

the transmitted power distribution is illustrated in Fig. 12-2-1. Observe that if $\Phi_{nn}(f)/|C(f)|^2$ is interpreted as the bottom of a bowl of unit depth, and we pour an amount of water equal to P_{av} into the bowl, the water will distribute itself in the bowl so as to achieve capacity. This is called the *water-filling interpretation* of the optimum power distribution as a function of frequency.

It is interesting to note that the channel capacity is the smallest when the channel SNR $|C(f)|^2/\Phi_{nn}(f)$ is a constant for all $f \in W$. In this case, $P(f)$ is a constant for all $f \in W$. Equivalently, if the channel frequency response is ideal, i.e., $C(f) = 1$ for $f \in W$, then the worst gaussian noise power distribution, from the viewpoint of maximizing capacity, is white gaussian noise.

The above development suggests that multicarrier modulation that divides the available channel bandwidth into subbands of relatively narrow width $\Delta f = W/N$ provides a solution that could yield transmission rates close to capacity. The signal in each subband may be independently coded and modulated at a synchronous symbol rate of $1/\Delta f$, with the optimum power allocation $P(f)$. If Δf is small enough then $C(f)$ is essentially constant across each subband, so that no equalization is necessary because the ISI is negligible.

Multicarrier modulation has been used in modems for both radio and telephone channels. Multicarrier modulation has also been proposed for future digital audio broadcast applications.

A particularly suitable application of multicarrier modulation is in digital transmission over copper wire subscriber loops. The typical channel attenuation characteristics for such subscriber lines are illustrated in Fig. 12-2-2. We

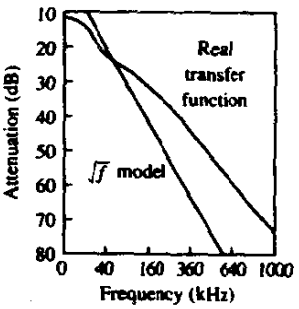

FIGURE 12-2-2 Attenuation characteristic of a 24 gauge 12 kft PIC loop. [*From Werner (1991) © IEEE.*]

observe that the attenuation increases rapidly as a function of frequency. This characteristic makes it extremely difficult to achieve a high transmission rate with a single modulated carrier and an equalizer at the receiver. The ISI penalty in performance is very large. On the other hand, multicarrier modulation with optimum power distribution provides the potential for a higher transmission rate.

The dominant noise in transmission over subscriber lines is crosstalk interference from signals carried on other telephone lines located in the same cable. The power distribution of this type of noise is also frequency-dependent, which can be taken into consideration in the allocation of the available transmitted power.

A design procedure for a multicarrier QAM system for a nonideal linear filter channel has been given by Kalet (1989). In this procedure, the overall bit rate is maximized, through the design of an optimal power division among the subcarriers and an optimum selection of the number of bits per symbol (sizes of the QAM signal constellations) for each subcarrier, under an average power constraint and under the constraint that the symbol error probabilities for all subcarriers are equal.

Below, we present an implementation of a multicarrier QAM modulator and demodulator that is based on the discrete Fourier transform (DFT) for the generation of the multiple carriers.

12-2-2 An FFT-Based Multicarrier System

In this section, we describe a multicarrier communication system that employs the fast Fourier transform (FFT) algorithm to synthesize the signal at the transmitter and to demodulate the received signal at the receiver. The FFT is simply the efficient computational tool for implementing the discrete fourier transform (DFT).

Figure 12-2-3 illustrates a block diagram of a multicarrier communication

FIGURE 12-2-3 Multicarrier communication system.

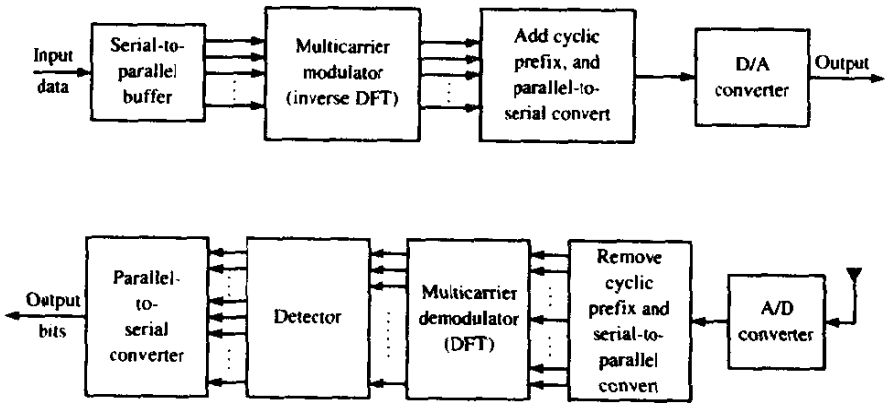

system. A serial-to-parallel buffer segments the information sequence into frames of N_f bits. The N_f bits in each frame are parsed into $\tilde{N}$ groups, where the ith group is assigned $\tilde{n}_i$ bits, and

$$\sum_{i=1}^{\tilde{N}} \tilde{n}_i = N_f \tag{12-2-9}$$

Each group may be encoded separately, so that the number of output bits from the encoder for the ith group is $n_i \geq \tilde{n}_i$.

It is convenient to view the multicarrier modulation as consisting of $\tilde{N}$ independent QAM channels, each operating at the same symbol rate $1/T$, but each channel having a distinct QAM constellation, i.e., the ith channel will employ $M_i = 2^{\tilde{n}_i}$ signal points. We denote the complex-valued signal points corresponding to the information symbols on the subchannels by X_k, $k = 0, 1, \ldots, \tilde{N} - 1$. In order to modulate the $\tilde{N}$ subcarriers by the information symbols $\{X_k\}$, we employ the inverse DFT (IDFT).

However, if we compute the $\tilde{N}$-point IDFT of $\{X_k\}$, we shall obtain a complex-valued time series, which is not equivalent to $\tilde{N}$ QAM-modulated subcarriers. Instead, we create $N = 2\tilde{N}$ information symbols by defining

$$X_{N-k} = X_k^*, \quad k = 1, \ldots, \tilde{N} - 1 \tag{12-2-10}$$

and $X_0' = \text{Re}\,(X_0)$, $X_{\tilde{N}} = \text{Im}\,(X_0)$. Thus, the symbol X_0 is split into two parts, both real. Then, the N-point IDFT yields the real-valued sequence

$$x_n = \frac{1}{\sqrt{N}} \sum_{k=0}^{N-1} X_k e^{j2\pi nk/N}, \quad n = 0, 1, \ldots, N - 1 \tag{12-2-11}$$

where $1/\sqrt{N}$ is simply a scale factor.

The sequence $\{x_n, 0 \leq n \leq N - 1\}$ corresponds to the samples of the sum $x(t)$ of $\tilde{N}$ subcarrier signals, which is expressed as

$$x(t) = \frac{1}{\sqrt{N}} \sum_{k=0}^{N-1} X_k e^{j2\pi kt/T}, \quad 0 \leq t \leq T \tag{12-2-12}$$

where T is the symbol duration. We observe that the subcarrier frequencies are $f_k = k/T$, $k = 0, 1, \ldots, \tilde{N}$. Furthermore, the discrete-time sequence $\{x_n\}$ in (12-2-10) represents the samples of $x(t)$ taken at times $t = nT/N$ where $n = 0, 1, \ldots, N - 1$.

The computation of the IDFT of the data $\{X_k\}$ as given in (12-2-10) may be viewed as multiplication of each data point X_k by a corresponding vector

$$\mathbf{v}_k = [v_{k0} \quad v_{k1} \quad \cdots \quad v_{k(N-1)}] \tag{12-2-13}$$

where

$$v_{kn} = \frac{1}{\sqrt{N}} e^{j(2\pi/N)kn} \tag{12-2-14}$$

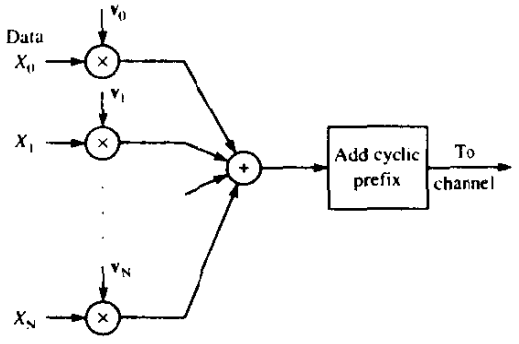

FIGURE 12-2-4 Signal synthesis for multicarrier modulation based on inverse DFT.

as illustrated in Fig. 12-2-4. In any case, the computation of the DFT is performed efficiently by the use of the FFT algorithm.

In practice, the signal samples $\{x_n\}$ are passed through a D/A converter whose output, ideally, would be the signal waveform $x(t)$. The output of the channel is the waveform

$$r(t) = x(t) \bigstar h(t) + n(t) \tag{12-2-15}$$

where $h(t)$ is the impulse response of the channel and $\bigstar$ denotes convolution. By selecting the bandwidth Δf of each subchannel to be very small, the symbol duration $T = 1/\Delta f$ is large compared with the channel time dispersion. To be specific, let us assume that the channel dispersion spans $\nu + 1$ signal samples where $\nu \ll N$. One way to avoid the effect of ISI is to insert a time guard band of duration $\nu T/N$ between transmissions of successive blocks.

An alternative method that avoids ISI is to append a cyclic prefix to each block of N signal samples $\{x_0, x_1, \ldots, x_{N-1}\}$. The cyclic prefix for this block of samples consists of the samples $x_{N-\nu}, x_{N-\nu+1}, \ldots, x_{N-1}$. These new samples are appended to the beginning of each block. Note that the addition of the cyclic prefix to the block of data increases the length of the block to $N + \nu$ samples, which may be indexed from $n = -\nu, \ldots, N-1$, where the first ν samples constitute the prefix. Then, if $\{h_n, 0 \leq n \leq \nu\}$ denotes the sampled channel impulse response, its convolution with $\{x_n, -\nu \leq n \leq N-1\}$ produces $\{r_n\}$, the received sequence. We are interested in the samples of $\{r_n\}$ for $0 \leq n \leq N-1$, from which we recover the transmitted sequence by using the N-point DFT for demodulation. Thus, the first ν samples of $\{r_n\}$ are discarded.

From a frequency-domain viewpoint, when the channel impulse response is $\{h_n, 0 \leq n \leq \nu\}$, its frequency response at the subcarrier frequencies $f_k = k/N$ is

$$H_k \equiv H\left(\frac{2\pi k}{N}\right) = \sum_{n=0}^{\nu} h_n e^{-j2\pi nk/N} \tag{12-2-16}$$

Due to the cyclic prefix, successive blocks (frames) of the transmitted

information sequence do not interfere and, hence, the demodulated sequence may be expressed as

$$\hat{X}_k = H_k X_k + \eta_k, \quad k = 0, 1, \ldots, N-1 \tag{12-2-17}$$

where $\{\hat{X}_k\}$ is the output of the N-point DFT demodulator, and η_k is the additive noise corrupting the signal. We note that by selecting $N \gg \nu$, the rate loss due to the cyclic prefix can be rendered negligible.

As shown in Fig. 12-2-3, the information is demodulated by computing the DFT of the received signal after it has been passed through an A/D converter. The DFT computation may be viewed as a multiplication of the received signal samples $\{r_n\}$ from the A/D converter by $\mathbf{v}_n^*$, where $\mathbf{v}_n$ is defined in (12-2-12). As in the case of the modulator, the DFT computation at the demodulator is performed efficiently by use of the FFT algorithm.

It is a simple matter to estimate and compensate for the channel factors $\{H_k\}$ prior to passing the data to the detector and decoder. A training signal consisting of either a known modulated sequence on each of the subcarriers or unmodulated subcarriers may be used to measure the $\{H_k\}$ at the receiver. If the channel parameters vary slowly with time, it is also possible to track the time variations by using the decisions at the output of the detector or the decoder, in a decision-directed fashion. Thus, the multicarrier system can be rendered adaptive.

Multicarrier QAM modulation of the type described above has been implemented for a variety of applications, including high-speed transmission over telephone lines, such as digital subscriber lines.

Other types of implementation besides the DFT are possible. For example, a digital filter bank that basically performs the DFT may be substituted for the FFT-based implementation when the number of subcarriers is small, e.g., $N \leq 32$. For a large number of subcarriers, e.g., $N > 32$, the FFT-based systems are computatively more efficient.

One limitation of the DFT-type modulators and demodulators arises from the relatively large sidelobes in frequency that are inherent in DFT-type filter banks. The first sidelobe is only 13 dB down from the peak at the desired subcarrier. Consequently, the DFT-based implementations are vulnerable to interchannel interference (ICI) unless a full cyclic prefix is used. If ICI is a problem, due to channel anomalies, one may resort to other types of digital filter banks that have much lower sidelobes. In particular, the class of multirate digital filter banks that have the perfect reconstruction property associated with wavelet-based filters appear to be an attractive alternative (see Tzannes *et al.*, 1994; Rizos *et al.*, 1994).

12-3 BIBLIOGRAPHICAL NOTES AND REFERENCES

Multichannel signal transmission is commonly used on time-varying channels to overcome the effects of signal fading. This topic is treated in some detail in Chapter 14, where we provide a number of references to published work. Of

particular relevance to the treatment of multichannel digital communications given in this chapter are the two publications by Price (1962a,b).

There is a large amount of literature on multicarrier digital communication systems. Such systems have been implemented and used for over 30 years. One of the earliest systems, described by Doeltz *et al.* (1957) and called Kineplex, was used for digital transmission in the HF band. Other early work on multicarrier system design has been reported in the papers by Chang (1966) and Saltzburg (1967). The use of the DFT for modulation and demodulation of multicarrier systems was proposed by Weinstein and Ebert (1971).

Of particular interest in recent years is the use of multicarrier digital transmission for data, facsimile, and video on a variety of channels, including the narrowband (4 kHz) switched telephone network, the 48 kHz group telephone band, digital subscriber lines, cellular radio, and audio broadcast. The interested reader may refer to the many papers in the literature. We cite as examples the papers by Hirosaki *et al.* (1981, 1986), Chow *et al.* (1991), and the survey paper by Bingham (1990). The paper by Kalet (1989) gives a design procedure for optimizing the rate in a multicarrier QAM system given constraints on transmitter power and channel characteristics. Finally, we cite the book by Vaidyanathan (1993) and the papers by Tzannes *et al.* (1994) and Rizos *et al.* (1994) for a treatment of multirate digital filter banks.

PROBLEMS

12-1 $X_1, X_2, \ldots, X_N$ are a set of N statistically independent and identically distributed real gaussian random variables with moments $E(X_i) = m$ and var $(X_i) = \sigma^2$.

a Define

$$U = \sum_{n=1}^{N} X_n$$

Evaluate the SNR of U, which is defined as

$$(\text{SNR})_U = \frac{[E(U)]^2}{2\sigma_U^2}$$

where σ_U^2 is the variance of U.

b Define

$$V = \sum_{n=1}^{N} X_n^2$$

Evaluate the SNR of V, which is defined as

$$(\text{SNR})_V = \frac{[E(V)]^2}{2\sigma_V^2}$$

where σ_V^2 is the variance of V.

c Plot $(\text{SNR})_U$ and $(\text{SNR})_V$ versus m^2/σ^2 on the same graph and, thus, compare the SNRs graphically.

d What does the result in (c) imply regarding coherent detection and combining versus square-law detection and combining of multichannel signals?

12-2 A binary communication system transmits the same information on two diversity channels. The two received signals are

$$r_1 = \pm\sqrt{\mathscr{E}_b} + n_1$$
$$r_2 = \pm\sqrt{\mathscr{E}_b} + n_2$$

where $E(n_1) = E(n_2) = 0$, $E(n_1^2) = \sigma_1^2$ and $E(n_2^2) = \sigma_2^2$, and n_1 and n_2 are uncorrelated gaussian variables. The detector bases its decision on the linear combination of r_1 and r_2, i.e.,

$$r = r_1 + kr_2$$

a Determine the value of k that minimizes the probability of error.

b Plot the probability of error for $\sigma_1^2 = 1$, $\sigma_2^2 = 3$, and either $k = 1$ or k is the optimum value found in (a). Compare the results.

12-3 Assess the cost of the cyclic prefix (used in multitone modulation to avoid ISI) in terms of

a extra channel bandwidth;

b extra signal energy.

12-4 Let $x(n)$ be a finite-duration signal with length N and let $X(k)$ be its N-point DFT. Suppose we pad $x(n)$ with L zeros and compute the $(N + L)$-point DFT, $X'(k)$. What is the relationship between $X(0)$ and $X'(0)$? If we plot $|X(k)|$ and $|X'(k)|$ on the same graph, explain the relationships between the two graphs.

12-5 Show that the sequence $\{x_n\}$ given by (12-2-11) corresponds to the samples of the signal $x(t)$ given by (12-2-12).

12-6 Show that the IDFT of a sequence $\{X_k, 0 \leq k \leq N-1\}$ can be computed by passing the sequence $\{X_k\}$ through a bank of N linear discrete-time filters with system functions

$$H_n(z) = \frac{1}{1 - e^{j2\pi n/N} z^{-1}}$$

12-7 Plot $P_2(L)$ for $L = 1$ and $L = 2$ as a function of $10 \log \gamma_b$ and determine the loss in SNR due to the combining loss for $\gamma_b = 10$.